Energy Conversion and Management 114 (2016) 197–208

Contents lists available at ScienceDirect

Energy Conversion and Management

journal homepage: www.elsevier.com/locate/enconman

# Wind speed forecasting using FEEMD echo state networks with RELM in Hebei, China

Wei Sun, Mohan Liu *

*Department of Business Administration, North China Electric Power University, Baoding 071000, China*

ARTICLE INFO

*Article history:*
Received 24 November 2015
Accepted 7 February 2016
Available online 18 February 2016

*Keywords:*
Short-term wind speed forecasting
Mid-term wind speed forecasting
FEEMD
RELM

ABSTRACT

Reducing the dependence on fossil-fuel-based resources is becoming significant due to the detrimental effects on environment and global energy-dependent. Thus, increased attention has been paid to wind power, a type of clean and renewable energy. However, owing to the stochastic nature of wind speed, it is essential to build a wind speed forecasting model with high-precision for wind power utilization. Therefore, this paper proposes a hybrid model which combines fast ensemble empirical model decomposition (FEEMD) with regularized extreme learning machine (RELM). The original wind speed series are first decomposed into a limited number of intrinsic mode functions (IMFs) and one residual series. Then RELM is built to forecast the sub-series. Partial auto correlation function (PACF) is applied to analyze the intrinsic relationships between the historical speeds so as to select the inputs of RELM. To verify the developed models, short-term wind speed data in July 2010 and monthly data from January 2000 to May 2010 in Hong songwa wind farm, Chengde city are used for model construction and testing. Two additional forecasting cases in Hebei province are also applied to prove the model's validity. The simulation test results show that the built model is effective, efficient and practicable.



## 1. Introduction

According to World Energy Outlook 2014, global energy demand will increase by 37% during 2014–2040 [1]. The acceleration of power structural adjustment is imperative because of the shortage of fossil fuels and environment degradation. In this case, wind energy, as the most technically mature and economically viable renewable resource, shows a promising potential of power structure improvement. At the end of 2014, the total wind energy reserves in China have reached $32.26 \times 10^6$ MW, and the installed wind power capacity has amounted to $95.81 \times 10^4$ MW [1]. In Hebei province, the wind energy industry has been booming over the past decade. According to the twelfth-five plan, the installed wind power capacity in Hebei province will reach over $1.1 \times 10^4$ MW in 2015 [2]. Based on the development strategy, the onshore wind power in Hebei province will increase to $1.64 \times 10^4$ MW by 2020.

Along with the increasingly high wind power penetration in Hebei province, it is necessary to improve the accuracy of wind speed prediction. Nowadays, scholars have published their important work to handle wind speed forecasting. These methods can be divided into four categories: physical modeling methods, time series models, artificial neural networks (ANNs) and hybrid methods. Physical models forecast the wind speed by utilizing physical parameters, such as temperature, pressure and surface roughness. These methods need large amount of computing time so that they are not suitable for short-term wind speed prediction. The numerical weather prediction (NWP) technology is the most commonly used physical model which applies mathematical models of the meteorological parameters to predict the wind speed. Al-Yahyai et al. [3] put up with nested ensemble NWP model for the wind resource assessment. The computational experiments showed that the nested ensemble NWP could predict the wind data very satisfactorily. Time series models, including vector autoregressive model [4] and autoregressive integrated moving average (ARIMA) [5–7], primarily forecast wind speed through analyzing historical data. Shukur and Lee [5] aimed at improving the accuracy of wind speed forecasting and combined ARIMA with ANN and kalman filter to handle the uncertain characteristic of wind speed. Yu et al. [6] outlined the models for long-term wind speed prediction and developed ARIMA based model to forecast wind speed. The results showed that the proposed model could meet the satisfaction of long-term wind speed forecasting. Guo et al. [7] put forward a

* Corresponding author at: Department of Business Administration, North China Electric Power University, 689 Huadian Road, Baoding 071000, China. Tel.: +86 15933961395.

*E-mail addresses:* bdsunwei@126.com (W. Sun), 1315289985@qq.com (M. Liu).

http://dx.doi.org/10.1016/j.enconman.2016.02.022
0196-8904/

hybrid seasonal auto-regression integrated moving average (SARIMA) and least square support vector machine (LSSVM) model to predict the mean monthly wind speed in Hexi Corridor. The study indicated that the accession of LSSVM significantly improved the computational performance of ARIMA. Many available papers including the ones discussed above have proposed that the nonlinear pattern of wind speed data is the important factor that affects the accuracy of ARIMA forecasting [8].

To improve the wind speed forecasting accuracy, ANNs build a non-linear function of high dimension to fit the historical wind speed. Jiang et al. [9] put up with a new method for forecasting wind speed in very short-term time scale by using Bayesian theory and structural break modeling. In ANN models, back propagation neural network (BPNN) [10,11], radial basis function (RBF) neural network [12–14], and extreme learning machine (ELM) [16–19] have been generally employed. Liu et al. [10] proposed a hybrid model for wind speed prediction. Four BPNN-based forecasting methods were introduced for the multi-step wind speed forecasting based on the adaptive boosting. Results showed that the hybrid model had good performance in terms of accuracy and consistency. Velo [11] applied BPNN to determine the annual average wind speed. Through multilayer perceptron with three layers, the proposed model obtained reliable estimations. In 2009, Chen et al. [12] successfully introduced RBF neural network into wind speed prediction. By using the orthogonal least squares algorithm, the inputs of the network were organized and their research revealed the effectiveness of the proposed approach. Shamshirband et al. [13] investigated RBF to forecast the wind speed for obtaining the optimal values of the wind turbine reaction torque. Li and Shi [14] proposed three different ANNs, namely adaptive linear element, BPNN, and RBF, for the wind speed predictions. The results indicated that RBF had better performance in mean absolute error, root mean square error, and mean absolute percentage error compared with other two methods. Through the studies above, BPNN and RBF neural network may cause model-inoperation when the data are not sufficient. To this end, Huang put up with ELM in 2004 [15]. ELM has faster convergence speed and less artificial interference which lead to strong generalization ability to heterogeneous data sets in comparison with the traditional neural networks. Based on the above advantages, ELM has been widely applied in forecasting. Wang [16] proposed a hybrid forecasting approach which combined ELM, Ljung-Box *Q*-test and SARIMA to ensure the accuracy of the mean daily and mean monthly wind speed forecasting. The results suggested the hybrid approach had better generality. Liu et al. [17] used ELM based probabilistic forecasting method for wind speed. With the historical wind power time series as the input alone, wind power forecasting was conducted in different steps by using the proposed model. The results indicated that the proposed hybrid model had satisfactory performance. Salcedo-Sanz et al. [18] applied ELM in short-term wind speed prediction and utilized coral reefs optimization algorithm and harmony search to optimize the input of ELM. The good results elaborated on the applicability of ELM in wind speed forecasting. Cancelliere et al. [19] collected wind speed data from Italy to develop ANN based prediction models. Among the comparisons, ELM showed the best performance while the BPNN showed the worst. Up to now, the advantages of ELM over traditional artificial networks are highlighted and also the uncertainties related to prediction are quantified via the bootstrapping technique. With lots of advantages such as fast training speed, high training accuracy, easy design process and no manual tuning, ELM can effectively obtain optimal solution. However, ELM is based on empirical risk minimization principle that easily causes over-fitting phenomenon. In order to improve the generalization capacity of ELM, this paper introduces a penalty factor to improve ELM and adopts RELM to forecast the wind speed. The algorithm takes the structural risk minimization into account and prevents over-fitting during the network training process by adjusting the size of the penalty factor and minimizing structural and empirical risk.

Based on the aforementioned discussion, it can be seen that the utilizations of the single methods make a certain restriction in wind speed forecasting. Thus, the hybrid methods are greatly developed to obtain a better wind speed forecasting performance. Salcedo-Sanz et al. [20] put forward a new hybridization of the fifth generation mesoscale model (MM5) with ANN to solve the problem of short-term wind speed prediction. Compared with single models, the hybrid method was able to achieve better satisfactory results. Similar hybrid models were proposed combining weather forecast model MM5 and banks of square support vector machines to improve precision [21]. Khashei et al. [22] presented a novel hybrid wind speed forecasting method based on ARIMA, fuzzy logic and ANNs. Fuzzy logic and ANNs were employed to overcome the linear and data limitations of ARIMA. Zhang et al. [23] successfully forecasted the short-term wind speed in the Gansu province in China based on a hybrid model which combined seasonal adjustment method with RBF. Kani and Ardehali [24] examined a time series method for very short-term wind speed forecasting. This time series forecasting model was on the basis of ANN and Markov chain, and the results indicated that the proposed hybrid method could obtain the better wind speed forecasting performance compared with the single methods. In the above-mentioned methods, the original data are usually directly applied as independent variables. Nevertheless, because of the chaotic nature and inherent complexity of wind speed, describing the movement tendency becomes difficult. Out of the purpose of constructing a stable prediction model, it is very necessary to make analysis of the original data features. Thus, the multi-scale decomposition of the original wind speed is indispensable in improving the prediction accuracy. The most common data preprocessing-based approaches, such as wavelet transform (WT) [25,26] and empirical mode decomposition (EMD) [27–29], are adopted to decompose the wind series and eliminate the stochastic volatility. Chitsaz et al. [25] executed a wind speed forecasting method based on clonal selection algorithm and wavelet neural network while WT was used to eliminate the irregular fluctuation of wind speed. De Giorgi et al. [26] put up with WT and LSSVM for short-term wind speed forecasting. Their study proved that the denoise processing was able to improve the prediction accuracy significantly. An et al. [27] came up with EMD, which was a signal filtering method, to improve the forecasting accuracy of multi-output feed forward neural network and gained a good effect. Ren et al. [28] built a hybrid EMD–ARIMA model for wind speed forecasting. The EMD was presented to improve the ability of the standard ARIMA model by coping with some jumping wind speed samplings. Liu et al. [29] designed a novel hybridization to predict wind speed by combining the EMD and the ANN. In this approach, EMD was used to decompose the original non-stationary wind speed into a series of sub-layers and ANN was conducted for forecasting all the sub-layers. The results proved that EMD could enhance the prediction precision. It is shown in the relevant documents that the selection of base wavelet and scale level may cause the false wave in WT decomposition while EMD has good self-adaptability and stable decomposition results in dealing with nonlinear and non-stationary data. However, the mode mixing problem in EMD greatly influences the results accuracy. Thus, aiming at this shortcoming, the ensemble empirical mode decomposition (EEMD) has been exploited by Huang in 2009 [30]. Comparing with EMD, EEMD has better performance in the decomposition of non-stationary signals. To further improve the real-time computational performance of EEMD, in 2014, Wang proposed a new decomposing algorithm named fast ensemble empirical mode decomposition (FEEMD) [31]. Many references indicate that FEEMD can predict the jumping wind speed samplings successfully. Liu et al. [32] combined FEEMD, genetic algorithm and ANN to establish a reliable wind speed forecasting approach. The authors proved that FEEMD could deal with the wind speed fluctuation efficiently. Therefore, in our study, the latest FEEMD is used to convert the original wind data into multiple empirical modes and EMD and WT are included in the performance comparison.

Most wind speed forecasting methodologies found above are used to forecast short-term wind speed or mid-term wind speed separately. Few combines both of them together. However, in practical work, the wind farm requires both short-term wind speed prediction to calculate short-term wind turbines output power and mid-term wind speed prediction to make wind farm development plans. In order to better meet the actual demand of wind farm, in this paper, a hybrid forecasting model based on RELM is built and the characteristics of short-term and mid-term wind speed are simultaneously considered.

This paper is organized as follows: Section 2 shows a brief description of FEEMD, ELM and RELM; Section 3 presents the frame work of the proposed technique while Section 4 pretreats the original short-term and mid-term wind speed; in Section 5, this paper analyzes the short-term and mid-term wind speed forecasting results of the proposed hybrid models; Section 6 provides two additional wind speed forecasting cases; and Section 7 concludes the paper based on the experimental results.

## 2. Methodology

### 2.1. Fast ensemble empirical mode decomposition

As an auxiliary signal processing method, EEMD incorporates Gaussian white noise into the original time series before applying multilevel signal decomposition via EMD, so as to uniformly distribute the entire time series in different scales to avoid frequency aliasing. After solving the mode mixing problem, EEMD is very appropriate for the non-stationary and non-linear signal decomposition. In order to improve the operating speed of EEMD, FEEMD was investigated by Wang in 2014 and the numerical examples [33,34] were presented to verify that FEEMD was, in fact, a computationally efficient method.

Two important parameters which used in FEEMD algorithm are the amplitude $k$ of white noise and the replicated times $M$ of EMD. This paper fully considers the empirical data and takes $k$ as 0.05–0.5 times and $M$ as 100. The specific steps of FEEMD are shown as follows:

(1) Add the random Gaussian white noise sequence $n_m(t)$ into the original time series $x_t$

$$x_m(t) = x(t) + n_m(t) \tag{1}$$

where $x_m(t)$ indicates the noise-added signal used in FEEMD of the $m$ th trial.

(2) Decompose the noise-added signal $x_m(t)$ into a series of IMFs $c_{i,m}(t)$, $i = 1, 2, \cdots, n$ and a residue $r_{n,m}(t)$ by using the EMD method.

(3) Add different white noise sequences and repeat step (1) to step (2) until $m = M$.

(4) Calculate the ensemble mean $c_i(t)$ of the $M$ trials for each IMF and the residue $r_n(t)$ by the following equations, respectively:

$$c_i(t) = \sum_{m=1}^{M} c_{i,m}(t)/M \tag{2}$$

$$r_n(t) = \sum_{m=1}^{M} r_{n,m}(t)/M \tag{3}$$

### 2.2. Extreme learning machine

The ELM is a novel and fast learning algorithm based on the modification of the traditional single-hidden layer feed-forward [15]. The significant advantage of ELM is that it randomly assigns the weights and thresholds between the inputting layer and the hidden layer and does not need to adjust these parameters during the learning process thus it can complete the training process extremely fast [35]. Besides learning velocity, ELM has better accuracy performance than other ANNs [36].

The structure of a standard ELM network is demonstrated in Fig. 1 and the working principle is shown as follow:

For given dataset $T = \{(x_1, t_1), (x_2, t_2), \cdots, (x_i, t_i)\}$ where $x_i = [x_{i1}, x_{i2}, \cdots, x_{in}]^T \in R^n$, $t_i = [t_{i1}, t_{i2}, \cdots, t_{im}]^T \in R^m$, set the activation function which contains $L$ hidden layer nodes as $g(x)$. The computational steps of the standard ELM are illustrated as follows:

(1) Randomize the bias between the input weights and the hidden layer of the given network as:

$$(a_i, b_i), \quad i = 1, 2, \cdots, L \tag{4}$$

(2) The feed forward neural network output of activation function $g(x)$ is expressed as:

$$f_L(x) = \sum_{i=1}^{L} \beta_i G(a_i * x_i + b_i), x, a_i \in R^n, \beta_i \in R^m \tag{5}$$

where the output matrix $H$ is shown as:

$$H(a_1, \cdots, a_L, b_1, \cdots, b_L, x_1, \cdots, x_N) = \begin{bmatrix} G(a_1 * x_1 + b_1) & \cdots & G(a_L * x_1 + b_L) \\ \vdots & \vdots & \vdots \\ G(a_1 * x_N + b_1) & \cdots & G(a_L * x_N + b_L) \end{bmatrix}_{N*L} \tag{6}$$

Thus formula (5) can be simplified as:

$$H\beta = Y \tag{7}$$

among it $\beta = \begin{bmatrix} \beta_1^T \\ \beta_2^T \\ \vdots \\ \beta_L^T \end{bmatrix}_{L*m}$ and $Y = \begin{bmatrix} y_1^T \\ y_2^T \\ \vdots \\ y_N^T \end{bmatrix}_{N*m}$.

(3) Output weight matrix $\beta$ can be obtained by the following formula:

$$\beta = H^+ Y \tag{8}$$

where $H^+$ represents generalized inverse matrix of hidden layer output matrix.

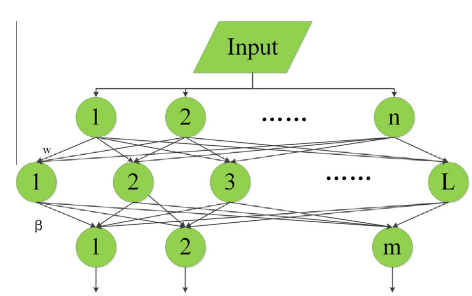


**Fig. 1.** Structure of the ELM network.

### 2.3. Regularized extreme learning machine

As mentioned above, ELM only considers empirical risk minimization and is prone to over-fitting [37]. Therefore, both empirical risk minimization and structural risk minimization should be taken into consideration when establishing a wind speed prediction model. The formula for calculation is shown as follows:

$$\min : \|\beta\|^2 + \sum_{i=1}^{N} \|\beta * h(x_i) - t_i\| \tag{9}$$

The defining equation can be expressed as:

$$\begin{aligned} &\min : L = \tfrac{1}{2}\left(\|\beta\|^2 + C\sum_{i=1}^{N}\|\xi_i\|^2\right) \\ &s.t. : h(x_i)\beta = t_i^T - \xi_i^T, \quad i = 1, 2, \cdots, N \end{aligned} \tag{10}$$

where $\xi_i$ represents the network output error corresponding to training sample $x_i$. According to Karush–Kuhn–Tucker condition, Lagrangian function is defined to solve the above optimization. Formula (10) is equivalent as:

$$\min : L_{RELM} = \frac{1}{2}\left(\|\beta\|^2 + C\sum_{i=1}^{N}\|\beta_i\|^2\right) - \sum_{i=1}^{N}\sum_{j=1}^{m}\alpha_{i,j}(h(x_i)\beta_j - t_{i,j} + \xi_{i,j}) \tag{11}$$

among it, the nonnegative $\alpha_i$ is Lagrange multiplier while $\beta_j$ represents the weights connected the hidden layer and the $j$ th output node. Set $\beta = [\beta_i, \cdots, \beta_m]$ and alter the formula (11) into:

$$\frac{\partial L_{RELM}}{\partial \beta_j} = 0 \rightarrow \beta_j = \sum_{i=1}^{N}\alpha_i h(x_i)^T \rightarrow \beta = H^T\alpha \tag{12}$$

$$\frac{\partial L_{RELM}}{\partial \xi_j} = 0 \rightarrow \alpha_i = C\xi_i, \quad i = 1, 2, \cdots, N \tag{13}$$

$$\frac{\partial L_{RELM}}{\partial \alpha_i} = 0 \rightarrow h(x_i)\beta \rightarrow t_i^T + \xi_i^T = 0, \quad i = 1, 2, \cdots, N \tag{14}$$

Substituting formula (12) and formula (13) into formula (14):

$$\begin{cases} h(x_1)H^TC\xi_1 - t_1^T + \xi_1^T = 0 \\ h(x_2)H^TC\xi_2 - t_2^T + \xi_2^T = 0 \\ \quad\vdots \\ h(x_N)H^TC\xi_N - t_N^T + \xi_N^T = 0 \end{cases} \tag{15}$$

Set $T = \begin{bmatrix} t_1^T \\ t_2^T \\ \vdots \\ t_N^T \end{bmatrix}$, $H = \begin{bmatrix} h(x_1) \\ h(x_2) \\ \vdots \\ h(x_N) \end{bmatrix}$, the above equation can be combined as follows:

$$\left(\frac{1}{C} + HH^T\right)\alpha = T \tag{16}$$

The output weight matrix $\beta$ can be calculated as:

$$\tilde{\beta} = H^T\left(HH^T + \frac{1}{C}\right)^{-1} T \tag{17}$$

among it, $\tilde{\beta}$ is the solution of $\beta$. Thus, the forecasting results of RELM is represented as:

$$f_L(x) = \sum_{i=1}^{L}\tilde{\beta}_i G(a_i * x_i + b_i) \tag{18}$$

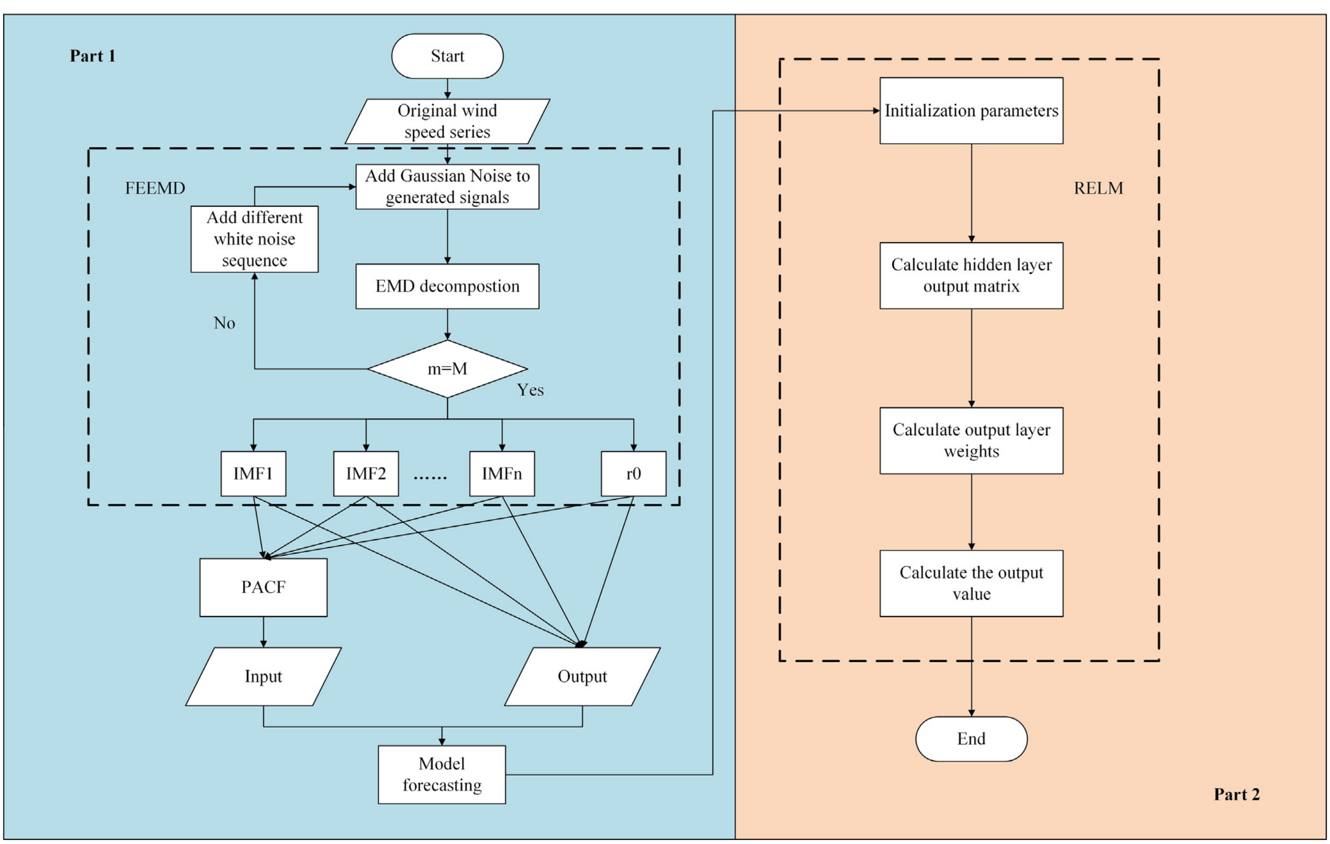


**Fig. 2.** The flowchart of FEEMD–RELM.


**Fig. 3.** The locations of the wind farms in Hebei province.

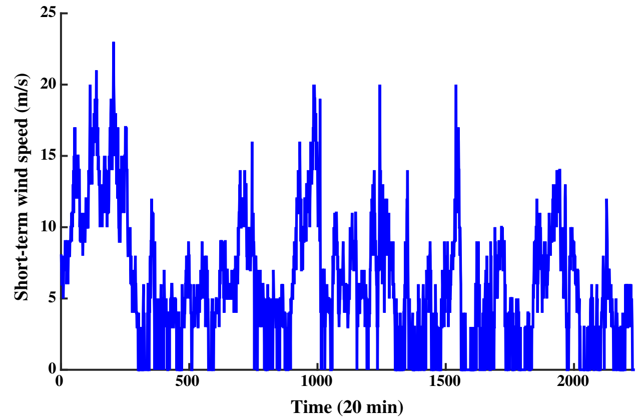


**Fig. 4.** Original short-term wind speed time series.

The comparison between ELM and RELM shows that, RELM inherits the simple parameter selection and fast training speed of ELM while adjusting the penalty factor to prevent over-fitting problems.

## 3. Approaches of FEEMD–RELM model

From the upper reviewing, it can be seen that, in the hybrid wind speed forecasting models, the decomposition algorithms are often applied to improve the forecasting accuracy of the proposed models. Thus, in this paper, FEEMD is put up with to enhance the forecasting performance of RELM. And in this section, the proposed method are discussed in detail. The flowchart of the FEEMD–RELM contains two parts, as Fig. 2 shows.

In Part 1, the original wind speed is decomposed into several IMFs with prominent local characteristics of the data and one residual series. As we discussed previously, the decomposition can accurately grasp the characteristics of the original information. The PACF analysis is employed to select historical wind speeds which have highest correlation on the target speed as the input of RELM model. After FEEMD pretreatment and the selection of input, the original wind data are divided into the training set and the test set. Part 2 aims at model validation. In this part, RELM are used to forecast the future wind speed.

## 4. Data preprocessing

In order to investigate the performance consistency of the proposed model with different wind datasets, this paper selects three representative wind farms in Hebei province to forecast the short-term and mid-term wind speed. The locations are shown in Fig. 3. For the purpose of reducing the repetition, this paper only describes wind speed forecasting in Hong songwa wind farm,

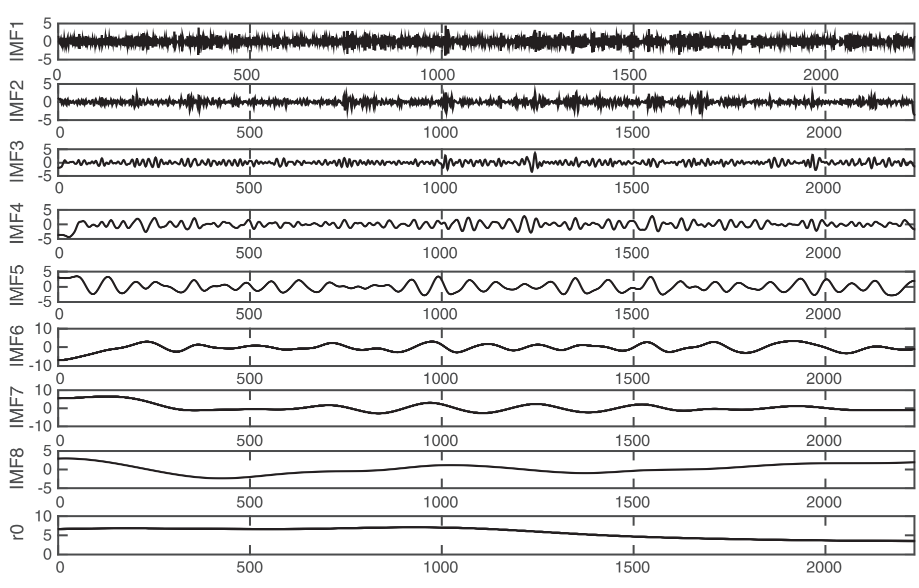


**Fig. 5.** The FEEMD decomposed results of original short-term wind speed time series.

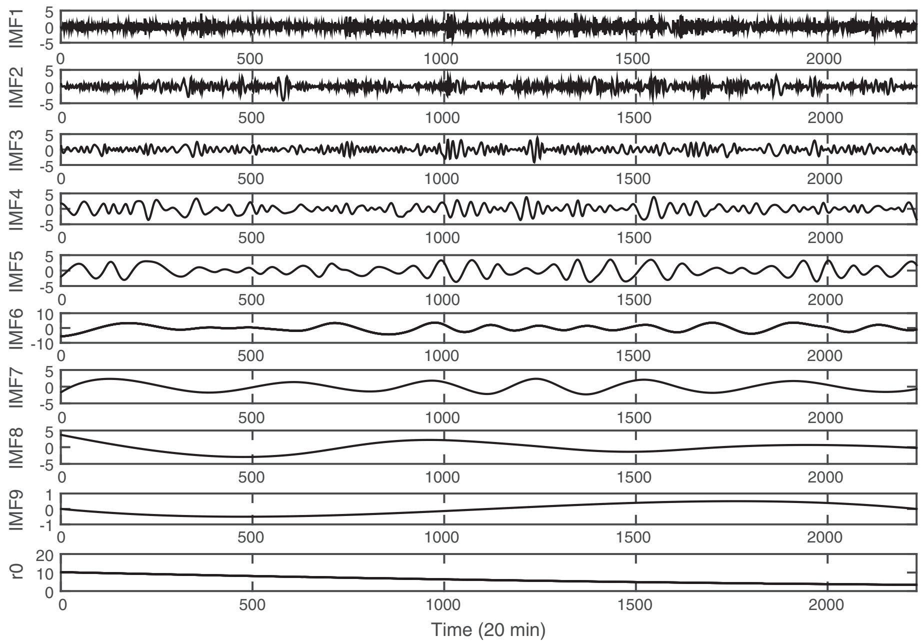


**Fig. 6.** The EMD decomposed results of original short-term wind speed time series.

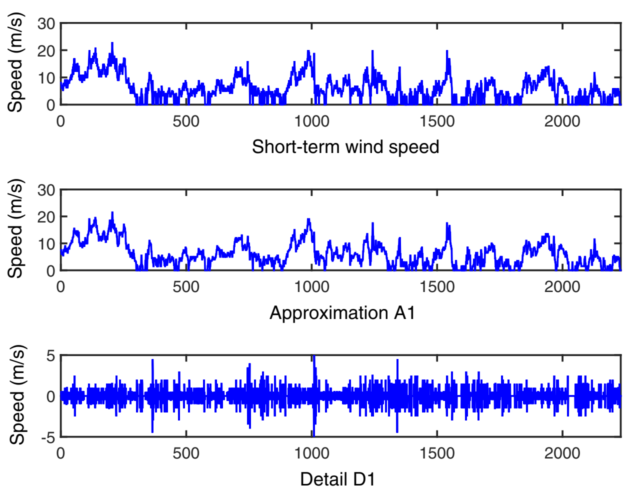


**Fig. 7.** The WT decomposed results of original short-term wind speed time series.

Chengde city in detail. The additional two sites are discussed in Section 6.

As an inland wind farm, Hong songwa wind farm is located in the transition zone of the southern edge of Inner Mongolia Plateau and northern mountain area of Hebei province, with a total area of 9219.72 square kilometers. For the purpose of demonstrating the efficiency of the proposed model in short-term and mid-term wind speed forecasting, this paper selects 20 min wind speed data in July 2010 and monthly wind speed data from January 2000 to May 2010 as samples in short-term and mid-term wind speed forecasting. Taking short-term wind speed data processing as example, Fig. 4 shows the 20 min wind speed time series in Hong songwa wind farm. In short-term wind speed forecasting, 2232 data from July 1, 2010 to July 31, 2010 are selected as training sample, and the remaining data from August 1 to August 3 are used as testing sample. The measuring height of the wind speed is 47 m.

### *4.1. Wind speed decomposition*

Fig. 4 shows that the short-term wind speed fluctuates severely. From the figure, we cannot see any apparent regularity of wind speed. Thus, FEEMD is exploited to decrease the non-stationary characteristic of the original short-term wind speed time series. The results are shown in Fig. 5, on which short-term wind speed is decomposed into 8 independent IMFs and one residue.

To further validate the effectiveness of the proposed method, EMD and WT are used as contrasts. The decompositions of short-term wind speed based on EMD method are shown in Fig. 6, on which EMD decomposes the short-term wind speed time series into 9 IMFs and one residue. Through the comparison between FEEMD, EMD decomposes the original wind speed into more layers which reduces the operation speed in some extent.

For highlighting the superiority of FEEMD, WT, a universal filter algorithm, is proposed to decompose the original wind speed time series into an approximation component $A_1$ and a detail component $D_1$. The approximation component is expected to present the main fluctuation of the wind speed while the detail component contains the spikes and stochastic volatilities. The results are shown in Fig. 7, on which $A_1$ offers a smooth form of the wind speed while $D_1$ depicts the high frequency components in the wind signal. So $A_1$ is taken as the wind speed to model for efficiency.

In mid-term wind speed forecasting, 123 average monthly wind speed data from January 2000 to May 2010 are used for the proposed model as the training set while a period of next five months are utilized as the testing set. Mid-term wind speed time series are measured in the same way as short-term wind speed, and the results are illustrated in Fig. 8. As it is shown in Fig. 8(a), similar with short-term wind speed fluctuation, mid-term wind speed is also needed to be decomposed by the FEEMD. As seen from Fig. 8 (b) and (c), the mid-term wind speed is decomposed into 4 IMFs and one residue by FEEMD and 5 IMFs and one residue by EMD. The decomposition results of mid-term wind speed via WT are similar to short-term wind speed, so $A_1$ is taken as input variable in the next forecasting step.

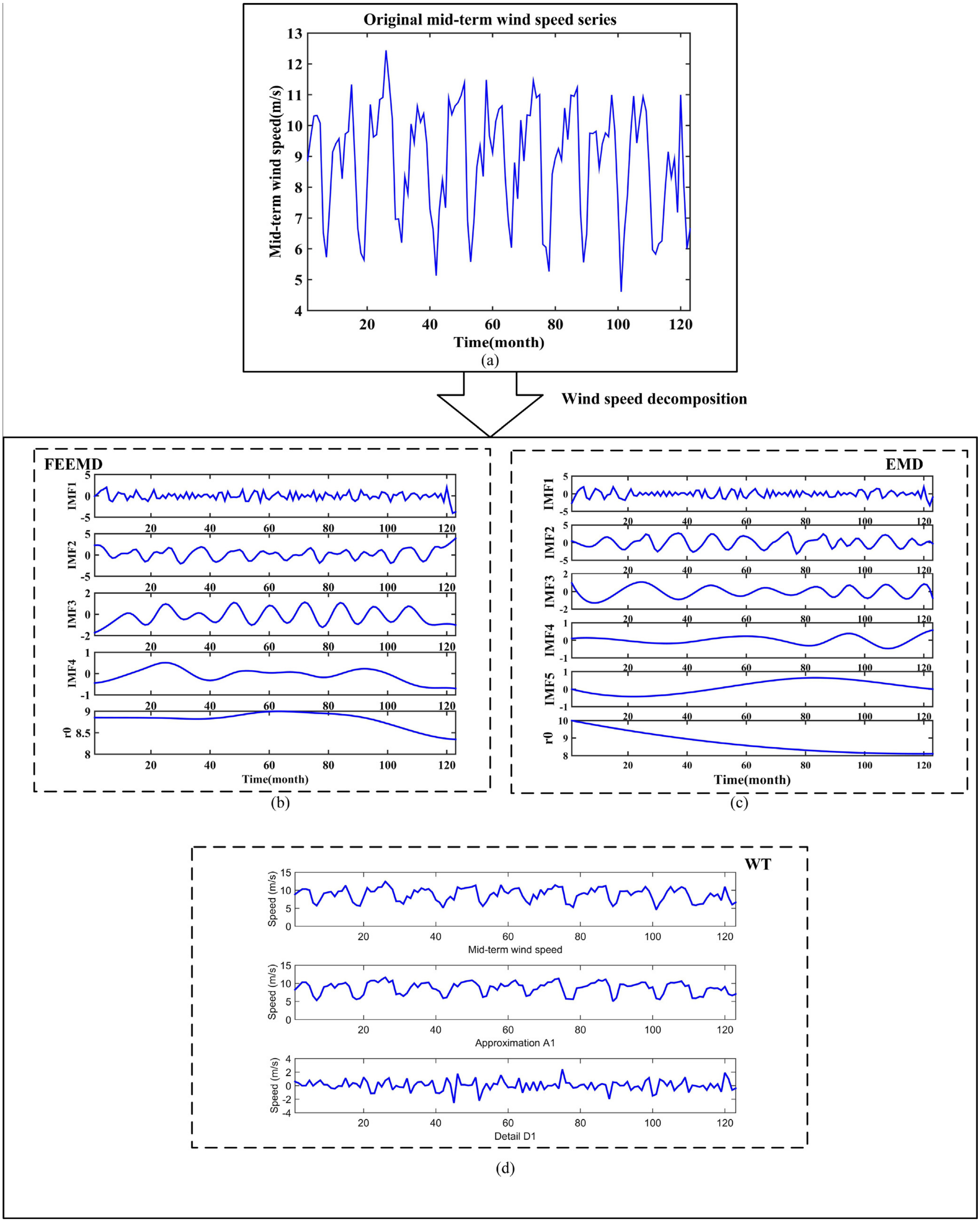


**Fig. 8.** The decomposed results of mid-term wind speed time series. (a) Original short-term wind speed time series. (b) The FEEMD decomposed results of original mid-term wind speed time series. (c) The EMD decomposed results of original mid-term wind speed time series. (d) The WT decomposed results of original mid-term wind speed time series.

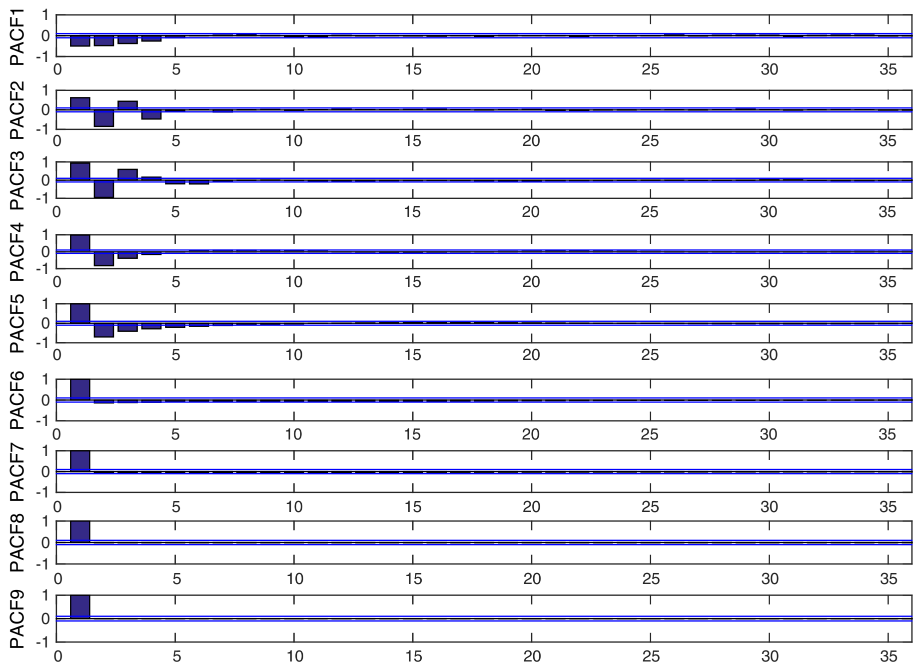


**Fig. 9.** PACF results of short-term wind speed decomposition after FEEMD.

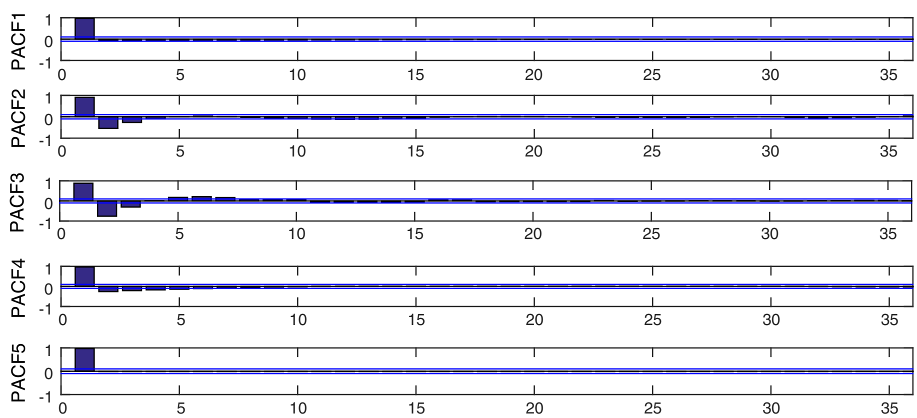


**Fig. 10.** PACF results of mid-term wind speed decomposition after FEEMD.

### *4.2. Input selection*

According to the tremendous influence of input variables selection to prediction results, PACF is investigated to derive the partial autocorrelogram of the obtained IMFs. Figs. 9 and 10 show the PACF results of short-term and mid-term wind speed data, respectively. Setting $x_i$ as the output variable, if the PACF at lag $k$ is out of the 95% confidence interval, $x_{i-k}$ is applied as one of the input variables. Table 1 shows input variables of the short-term and mid-term wind speed data for RELM obviously.

Through the same calculation, the lags of PACF after EMD and WT are shown in Table 2.

**Table 1**
Analysis of short-term and mid-term wind speed PACF results after FEEMD.

| Short-term wind speed | | Mid-term wind speed | |
|---|---|---|---|
| IMFs and $r_0$ | Lag | IMFs and $r_0$ | Lag |
| IMF1 | $(x_{t-1}, x_{t-2}, x_{t-3}, x_{t-4})$ | IMF1 | $(x_{t-1})$ |
| IMF2 | $(x_{t-1}, x_{t-2}, x_{t-3}, x_{t-4})$ | IMF2 | $(x_{t-1}, x_{t-2}, x_{t-3})$ |
| IMF3 | $(x_{t-1}, x_{t-2}, x_{t-3}, x_{t-4}, x_{t-5})$ | IMF3 | $(x_{t-1}, x_{t-2}, x_{t-3})$ |
| IMF4 | $(x_{t-1}, x_{t-2}, x_{t-3}, x_{t-4})$ | IMF4 | $(x_{t-1}, x_{t-2}, x_{t-3}, x_{t-4})$ |
| IMF5 | $(x_{t-1}, x_{t-2}, x_{t-3}, x_{t-4}, x_{t-5})$ | $r_0$ | $(x_{t-1})$ |
| IMF6 | $(x_{t-1}, x_{t-2})$ | | |
| IMF7 | $(x_{t-1}, x_{t-2})$ | | |
| IMF8 | $(x_{t-1})$ | | |
| $r_0$ | $(x_{t-1})$ | | |

## 5. Case studies

### *5.1. Model performance evaluation*

To effectively compare those models, three generally adopted error criteria are presented to measure the accuracy of all involved models, including coefficient of determination $R^2$, mean absolute percentage error (MAPE) and mean absolute error (MAE). Within the range [0, 1], the closer $R^2$ to 1, the better performance of the model. MAPE can measure the average forecasting ability of the model at each data points while the MAE is introduced to weigh the proximity between the actual value and the predicted value. The formulas of the above indexes are shown as below:

**Table 2**
Analysis of short-term and mid-term wind speed PACF results after EMD and WT.

| Short-term wind speed | | | | Mid-term wind speed | | | |
|---|---|---|---|---|---|---|---|
| EMD | | WT | | EMD | | WT | |
| IMF1 | $(x_{t\text{-}1}, x_{t\text{-}2}, x_{t\text{-}3})$ | $A_1$ | $(x_{t\text{-}1}, x_{t\text{-}2}, x_{t\text{-}3}, x_{t\text{-}4})$ | IMF1 | $(x_{t\text{-}1}, x_{t\text{-}2})$ | $A_1$ | $(x_{t\text{-}1}, x_{t\text{-}2})$ |
| IMF2 | $(x_{t\text{-}1}, x_{t\text{-}2}, x_{t\text{-}3}, x_{t\text{-}4})$ | | | IMF2 | $(x_{t\text{-}1}, x_{t\text{-}2}, x_{t\text{-}3})$ | | |
| IMF3 | $(x_{t\text{-}1}, x_{t\text{-}2}, x_{t\text{-}3}, x_{t\text{-}4}, x_{t\text{-}5})$ | | | IMF3 | $(x_{t\text{-}1}, x_{t\text{-}2})$ | | |
| IMF4 | $(x_{t\text{-}1}, x_{t\text{-}2}, x_{t\text{-}3}, x_{t\text{-}4}, x_{t\text{-}5}, x_{t\text{-}6})$ | | | IMF4 | $(x_{t\text{-}1}, x_{t\text{-}2}, x_{t\text{-}3}, x_{t\text{-}4})$ | | |
| IMF5 | $(x_{t\text{-}1}, x_{t\text{-}2}, x_{t\text{-}3}, x_{t\text{-}4})$ | | | IMF5 | $(x_{t\text{-}1}, x_{t\text{-}2}, x_{t\text{-}3})$ | | |
| IMF6 | $(x_{t\text{-}1}, x_{t\text{-}2}, x_{t\text{-}3})$ | | | $r_0$ | $(x_{t\text{-}1}, x_{t\text{-}2})$ | | |
| IMF7 | $(x_{t\text{-}1}, x_{t\text{-}2}, x_{t\text{-}3}, x_{t\text{-}4})$ | | | | | | |
| IMF8 | $(x_{t\text{-}1}, x_{t\text{-}2}, x_{t\text{-}3}, x_{t\text{-}4}, x_{t\text{-}5})$ | | | | | | |
| IMF9 | $(x_{t\text{-}1}, x_{t\text{-}2})$ | | | | | | |
| $r_0$ | $(x_{t\text{-}1}, x_{t\text{-}2})$ | | | | | | |

$$R^2 = \frac{\left(l\sum_{i=1}^{l}\hat{y}_i y_i - \sum_{i=1}^{l}\hat{y}_i \sum_{i=1}^{l} y_i\right)^2}{\left(l\sum_{i=1}^{l}\hat{y}_i^2 - \left(\sum_{i=1}^{l}\hat{y}_i\right)^2\right)\left(l\sum_{i=1}^{l}y_i^2 - \left(\sum_{i=1}^{l}y_i\right)^2\right)} \tag{19}$$

$$\text{MAPE} = \frac{1}{l}\sum_{i=1}^{l}\left|\frac{y_i - \hat{y}_i}{y_i}\right| * 100\% \tag{20}$$

$$\text{MAE} = \frac{1}{l}\sum_{i=1}^{l}|y_i - \hat{y}_i| \tag{21}$$

where $l$ is the number of testing samples while $y_i$ ($i = 1, 2, \cdots, l$) and $\hat{y}_i(i = 1, 2, \cdots, l)$ represent the $i$ th actual value and predictive value respectively.

In order to prominent the faster calculation speed of RELM compared with other ANNs, this paper contrasts the calculation speed t of the single ANN models under the same computing environment.

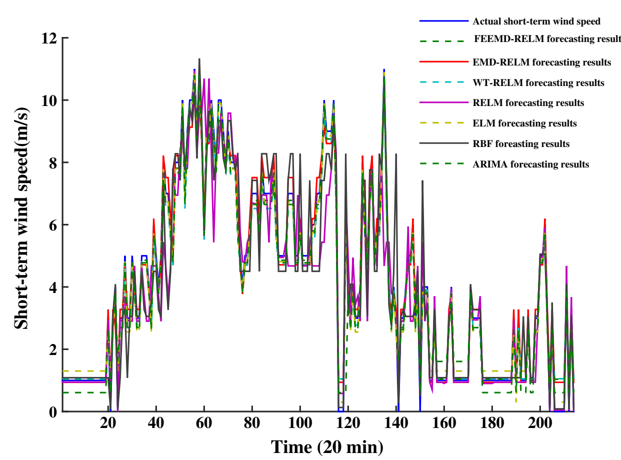


**Fig. 12.** The results of 8 models in the short-term wind speed forecasting.

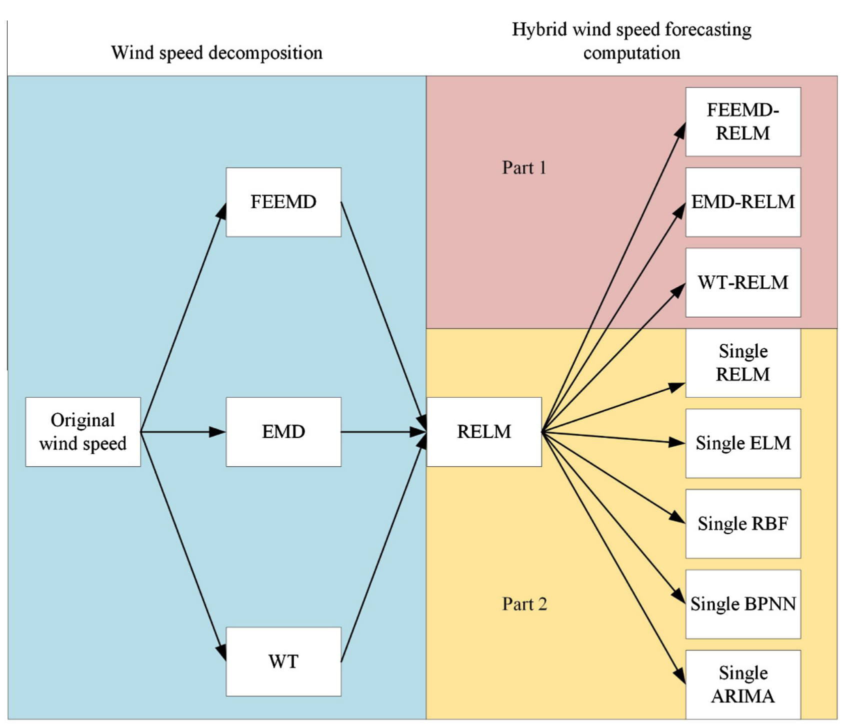


**Fig. 11.** Framework of the forecasting model comparisons.

**Table 3**
Analysis of short-term wind speed forecasting results.

| Index | FEEMD–RELM | EMD–RELM | WT–RELM | RELM | ELM | RBF | BPNN | ARIMA |
|---|---|---|---|---|---|---|---|---|
| $R^2$ (m/s) | 0.992 | 0.991 | 0.982 | 0.990 | 0.972 | 0.883 | 0.857 | 0.881 |
| MAPE (%) | 11.142 | 12.429 | 12.581 | 14.954 | 15.448 | 16.272 | 17.312 | 20.635 |
| MAE (m/s) | 0.214 | 0.287 | 0.305 | 0.289 | 0.397 | 0.461 | 0.483 | 0.582 |

**Table 4**
Computing time of RELM, ELM, RBF and BPNN in short-term wind speed forecasting.

| | RELM | ELM | RBF | BPNN |
|---|---|---|---|---|
| $t$ (s) | 5.77 | 5.53 | 24.72 | 25.12 |

### 5.2. Short-term wind speed forecasting

As Fig. 11 shows, the comparisons can be divided into two parts. The prior one is investigated to illustrate the advancement of FEEMD while the second part can verify the efficiency of RELM in wind speed forecasting. What's more, the contrast between the two parts can show that the introduction of decomposition is helpful to promote the accuracy of the forecasting models.

Fig. 12 shows the short-term wind speed prediction curves achieved by eight different models. The analysis shows that: (a) compared with other 7 models, the goodness of fit between the predicted value by FEEMD–RELM and actual value reaches the highest degree while ARIMA presents the lowest one; (b) at the jumping points of wind speed, the prediction accuracy of RELM is higher than ELM, which indicates that through the regularization improvement, the sensitivity of RELM has been strengthened; (c) the hybrid models have better predicted precision than the corresponding single format. It means that the FEEMD, EMD and WT decomposition afford good results in improving the forecasting performance of the single RELM.

The estimated results of the 8 predictions are given in Table 3. It can be concluded from the table that: (a) FEEMD–RELM shows the best performance while the BPNN shows the worst. This is because the inherent characteristics of BPNN may cause the low efficiency and local optimum. Furthermore, the selection of BPNN hidden nodes number highly depends on trial and error procedure. As a consequence, it is difficult to obtain the optimal network. The fitting degree of ARIMA is increasing along with the large training set, therefore in the short term wind speed forecasting, the performance of ARIMA model is slightly better than BPNN; (b) based on MAPE and MAE criteria, FEEMD is able to portray the dynamic behavior of short-term wind speed. The prediction accuracy of FEEMD–RELM has no relationship with time scale thus can lead to practical forecasting results. In addition, single models performance are inferior to the hybrid models, for example, the MAPE of RELM is 14.954% which is higher than the MAPE of FEEMD–RELM, EMD–RELM and WT–RELM. Although the MAE of RELM is higher than FEEMD–RELM and EMD–RELM about 0.75 m/s and 0.02 m/s, respectively, it is lower than WT–RELM about 0.16 m/s. Due to the positive and negative oscillations of wavelet coefficients around singular points, the degree of difficulty of singularity extraction and signal construction increases; (c) the $R^2$, MAPE and MAE of FEEMD–RELM and EMD–RELM are superior to WT–RELM. The wavelet transform of time-frequency is based on constraints of regularity, which has no self-adaptability. However, as an adaptive signal processing method, EMD has better advantages in dealing with non-stationary and nonlinear data; (d) the MAPE of FEEMD based prediction model is lower than EMD–RELM to 1.287%. The reason is that the Gaussian white noise of FEEMD has a statistical characteristic of uniform frequency distribution thus can solve mode mixing problem faced by EMD; (e) RELM

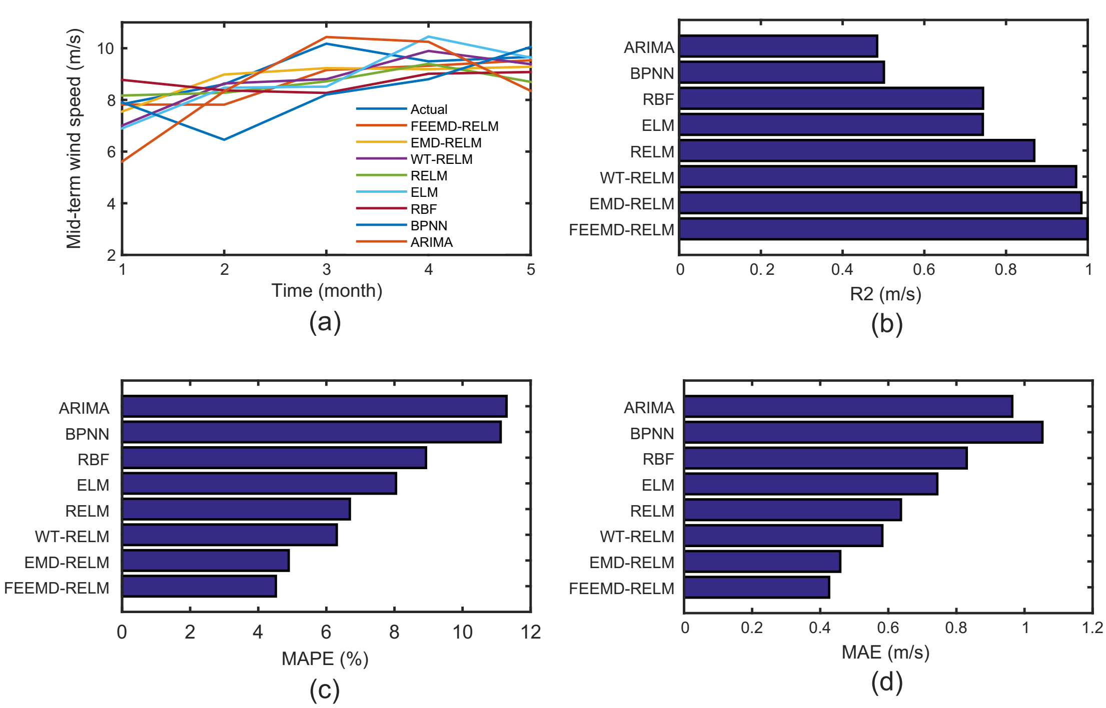


**Fig. 13.** Analysis of mid-term wind speed forecasting. (a) The results of 8 models in the mid-term wind speed forecasting. (b) The $R^2$ of 8 models in the mid-term wind speed forecasting. (c) The MAPE of 8 models in the mid-term wind speed forecasting. (d) The MAE of 8 models in the mid-term wind speed forecasting.

has the most outstanding performances in single models comparisons. RELM retains the superior generalization ability of ELM, meanwhile, regularization reduces the over-fitting of ELM. Compared with RBF and BPNN, ELM randomly generates the threshold of hidden layer neuron and the connection weights between the input layers and the hidden layers, therefore, avoiding the weight value setting faced by other ANNs.

Computing time of RELM, ELM, RBF and BPNN in short-term wind speed forecasting is shown in Table 4.

Table 4 shows that, the computing time of RELM and ELM are far shorter than RBF and BPNN which indicate that the high speed of ELM based models is achieved. This is because the randomly selected parameters are never updated during the whole learning process. The computing time of RELM is 0.24 s longer than the ELM one, thus indicates the regularization improvement has little influence on the running speed of ELM. Through the discussion of the prediction accuracy, it is clear that RELM preserves the fast running while improving the forecasting precision of ELM.

### 5.3. Mid-term wind speed forecasting

To further demonstrate the performance and extensive use of the proposed model, mid-term wind speed data in Hong songwa wind farm are provided in this study. The forecasting results of mid-term wind speed are presented in Fig. 13 and the computing time of the single ANNs are shown in Table 5. From Fig. 13, some similar conclusions can be made as follows: (a) in Fig. 13(a), ARIMA and BPNN show no constant changes while FEEMD–RELM has the highest fitting degree; (b) from Fig. 13(b) and (c), it can be seen that the $R^2$ of FEEMD–RELM is significantly higher than other models and the MAPE of RELM based models are all below 8%. It proves that RELM can precisely perform the non-linear change of mid-term wind speed and provide some practical value to wind speed forecasting; (c) the RELM has better forecasting performance than other ANNs and all the hybrid models have better performance than the single ones.

Table 5 shows that RELM can shorten calculation time, raise the efficiency of mathematical model and heighten the accuracy of mid-term wind speed forecasting.

**Table 5**
Computing time of RELM, ELM, RBF and BPNN in mid-term wind speed forecasting.

| | RELM | ELM | RBF | BPNN |
|---|---|---|---|---|
| $t$ (s) | 4.31 | 4.57 | 17.39 | 18.42 |

## 6. Additional forecasting cases

To future investigate the performance of the proposed model, two additional sites are applied in our paper, the particular content is shown in Table 6.

The proposed model is applied to predict the short-term and mid-term wind speed of the additional two sites in this study. The forecasting results of these additional two cases are presented in Tables 7 and 8, and the conclusions are similar to the ones which made in Section 5. Among the eight models used for forecasting, the ARIMA performs the worst and the FEEMD–RELM performs

**Table 6**
The particular content of two additional sites.

| Wind farm | Altitude (m) | Training set | | Test set | |
|---|---|---|---|---|---|
| | | Short-term wind speed | Mid-term wind speed | Short-term wind speed | Mid-term wind speed |
| Shang Yi wind farm | 29 | May 2010 | Oct. 2000–Dec. 2010 | Apr. 1st 2010–Apr. 3rd 2010 | Jan. 2011–May 2011 |
| Pu Ti wind farm | 30 | Nov. 2009 | Apr. 2001–Jul 2010 | Dec. 1st 2009–Dec. 3rd 2009 | Aug. 2010–Dec. 2010 |

**Table 7**
Analysis of short-term and mid-term wind speed forecasting results in Pu ti wind farm.

| | $R^2$ (m/s) | | MAPE (%) | | MAE (m/s) | |
|---|---|---|---|---|---|---|
| | Short-term | Mid-term | Short-term | Mid-term | Short-term | Mid-term |
| FEEMD–RELM | 0.934 | 0.989 | 10.271 | 4.813 | 0.559 | 0.181 |
| EMD–RELM | 0.904 | 0.972 | 11.804 | 5.910 | 0.795 | 0.226 |
| WT–RELM | 0.895 | 0.963 | 12.767 | 7.951 | 0.823 | 0.296 |
| RELM | 0.875 | 0.973 | 13.902 | 9.514 | 0.898 | 0.399 |
| ELM | 0.880 | 0.953 | 15.007 | 10.425 | 0.955 | 0.429 |
| RBF | 0.858 | 0.832 | 15.961 | 13.048 | 1.078 | 0.470 |
| BPNN | 0.849 | 0.593 | 16.925 | 14.167 | 1.093 | 0.614 |
| ARIMA | 0.749 | 0.278 | 19.171 | 16.336 | 1.184 | 0.722 |

**Table 8**
Analysis of short-term and mid-term wind speed forecasting results in Shang yi wind farm.

| | $R^2$ (m/s) | | MAPE (%) | | MAE (m/s) | |
|---|---|---|---|---|---|---|
| | Short-term | Mid-term | Short-term | Mid-term | Short-term | Mid-term |
| FEEMD–RELM | 0.908 | 0.909 | 10.684 | 6.218 | 1.149 | 0.363 |
| EMD–RELM | 0.883 | 0.886 | 12.092 | 8.466 | 1.323 | 0.531 |
| WT–RELM | 0.878 | 0.810 | 12.612 | 9.686 | 1.363 | 0.601 |
| RELM | 0.866 | 0.661 | 13.296 | 10.580 | 1.394 | 0.688 |
| ELM | 0.851 | 0.668 | 13.671 | 11.308 | 1.460 | 0.716 |
| RBF | 0.851 | 0.689 | 14.143 | 11.850 | 1.496 | 0.708 |
| BPNN | 0.827 | 0.613 | 14.950 | 13.110 | 1.595 | 0.788 |
| ARIMA | 0.820 | 0.618 | 17.145 | 14.973 | 1.720 | 0.884 |

best. The results manifest that the proposed model is effective in forecasting the short-term and mid-term wind speed series.

## 7. Conclusions

This paper proposes FEEMD-based decomposition with RELM-based forecaster for short-term and mid-term wind speed forecasting. Due to the volatility of wind speed, FEEMD is used in filtering process and then RELM is exploited to forecast the decomposed components. PACF is employed to choose the lags of the historical speeds as the inputs of RELM. The forecasting results indicate that the proposed model is effective and efficient for the short-term and mid-term wind speed prediction.

Base on the short-term and mid-term wind speed forecasting results in this paper, several conclusions can be obtained as follows: (a) combining FEEMD and RELM is an innovation practice for predicting the non-stationary and nonlinear wind speed time series; (b) the ELM based algorithms possess tuning-free operation thus can easily put into effect in wind farms; (c) compared with other decomposing algorithms in the hybrid models, FEEMD has the best performance while WT has the poorest; (d) the RELM based model can improve calculation efficiency with no loss in accuracy; (e) the proposed model outperforms other methods both in short-term and mid-term wind speed forecasting, thus greatly expands the application of the model and meets the demands of the wind farm.

Although the proposed model has obvious advantages in short-term and mid-term wind speed forecasting, the factors such as humidity, pressure and temperature have great influence on wind speed. However, this paper only analyzed unilabiate wind speed time series, other factors are excluded from the proposed hybrid model. The next study is to incorporate these factors and verify the developed hybrid approach.

## References


[1] Sieminski, A. International Energy Outlook, Energy Information Administration (EIA); 2014.
[2] Liu ZB. Wind power industry competitiveness evaluation in Hebei province based on improved fuzzy comprehensive evaluation model. Appl Mech Mater 2013:2567–70. Trans Tech Publ.
[3] Al-Yahyai S, Charabi Y, Al-Badi A, Gastli A. Nested ensemble NWP approach for wind energy assessment. Renewable Energy 2012;37:150–60.
[4] Sun CS, Wang YN, Li XR. A vector autoregression model of hourly wind speed and its applications in hourly wind speed forecasting. Proc – Chin Soc Electr Eng 2008;28:112.
[5] Shukur OB, Lee MH. Daily wind speed forecasting through hybrid KF-ANN model based on ARIMA. Renewable Energy 2015;76:637–47.
[6] Yu J, Chen K, Mori J, Rashid MM. A Gaussian mixture copula model based localized Gaussian process regression approach for long-term wind speed prediction. Energy 2013;61:673–86.
[7] Guo Z, Zhao J, Zhang W, Wang J. A corrected hybrid approach for wind speed prediction in Hexi Corridor of China. Energy 2011;36:1668–79.
[8] Liu H, Shi J, Erdem E. Prediction of wind speed time series using modified Taylor Kriging method. Energy 2010;35:4870–9.
[9] Jiang Y, Song Z, Kusiak A. Very short-term wind speed forecasting with Bayesian structural break model. Renewable Energy 2013;50:637–47.
[10] Liu H, Tian H-Q, Li Y-F, Zhang L. Comparison of four Adaboost algorithm based artificial neural networks in wind speed predictions. Energy Convers Manage 2015;92:67–81.
[11] Velo R, López P, Maseda F. Wind speed estimation using multilayer perceptron. Energy Convers Manage 2014;81:1–9.
[12] Chen B, Zhao L, Wang X, Lu JH, Liu GY, Cao RF, et al. Wind speed prediction using OLS algorithm based on RBF neural network. Asia-Pacific Power and Energy Engineering Conference (APPEEC), IEEE; 2009. p. 1–4.
[13] Shamshirband S, Petković D, Amini A, Anuar NB, Nikolić V, Ćojbašić Ž, et al. Support vector regression methodology for wind turbine reaction torque prediction with power-split hydrostatic continuous variable transmission. Energy 2014;67:623–30.
[14] Li G, Shi J. On comparing three artificial neural networks for wind speed forecasting. Appl Energy 2010;87:2313–20.
[15] Huang GB, Zhu QY, Siew CK. Extreme learning machine: a new learning scheme of feedforward neural networks. In: Proceedings of the international joint conference on neural networks, IEEE; 2004. p. 985–90.
[16] Wang J, Hu J, Ma K, Zhang Y. A self-adaptive hybrid approach for wind speed forecasting. Renewable Energy 2015;78:374–85.
[17] Liu H, Tian HQ, Li YF. Four wind speed multi-step forecasting models using extreme learning machines and signal decomposing algorithms. Energy Convers Manage 2015;100:16–22.
[18] Salcedo-Sanz S, Pastor-Sánchez A, Del Ser J, Prieto L, Geem Z. A coral reefs optimization algorithm with harmony search operators for accurate wind speed prediction. Renewable Energy 2015;75:93–101.
[19] Cancelliere R, Gosso A, Grosso A. Neural networks for wind power generation forecasting: a case study. In: 10th International conference on networking, sensing and control (ICNSC), IEEE; 2013. p. 666–71.
[20] Salcedo-Sanz S, Pérez-Bellido ÁM, Ortiz-García EG, Portilla-Figueras A, Prieto L, Paredes D. Hybridizing the fifth generation mesoscale model with artificial neural networks for short-term wind speed prediction. Renewable Energy 2009;34:1451–7.
[21] Ortiz-García EG, Salcedo-Sanz S, Pérez-Bellido ÁM, Gascón-Moreno J, Portilla-Figueras JA, Prieto L. Short-term wind speed prediction in wind farms based on banks of support vector machines. Wind Energy 2011;14:193–207.
[22] Khashei M, Bijari M, Ardali GAR. Improvement of auto-regressive integrated moving average models using fuzzy logic and artificial neural networks (ANNs). Neurocomputing 2009;72:956–67.
[23] Zhang W, Wang J, Wang J, Zhao Z, Tian M. Short-term wind speed forecasting based on a hybrid model. Appl Soft Comput 2013;13:3225–33.
[24] Kani SP, Ardehali M. Very short-term wind speed prediction: a new artificial neural network–Markov chain model. Energy Convers Manage 2011;52:738–45.
[25] Chitsaz H, Amjady N, Zareipour H. Wind power forecast using wavelet neural network trained by improved Clonal selection algorithm. Energy Convers Manage 2015;89:588–98.
[26] De Giorgi MG, Congedo PM, Malvoni M, Laforgia D. Error analysis of hybrid photovoltaic power forecasting models: a case study of mediterranean climate. Energy Convers Manage 2015;100:117–30.
[27] An N, Zhao W, Wang J, Shang D, Zhao E. Using multi-output feedforward neural network with empirical mode decomposition based signal filtering for electricity demand forecasting. Energy 2013;49:279–88.
[28] Ren Y, Suganthan P, Srikanth N. A comparative study of empirical mode decomposition-based short-term wind speed forecasting methods. IEEE Trans Sustain Energy 2015;6:236–44.
[29] Liu H, Chen C, Tian HQ, Li YF. A hybrid model for wind speed prediction using empirical mode decomposition and artificial neural networks. Renewable Energy 2012;48:545–56.
[30] Wu Z, Huang NE. Ensemble empirical mode decomposition: a noise-assisted data analysis method. Adv Adapt Data Anal 2009;1:1–41.
[31] Wang YH, Yeh CH, Young HWV, Hu K, Lo MT. On the computational complexity of the empirical mode decomposition algorithm. Physica A 2014;400:159–67.
[32] Liu H, Tian HQ, Liang XF, Li YF. New wind speed forecasting approaches using fast ensemble empirical model decomposition, genetic algorithm, mind evolutionary algorithm and artificial neural networks. Renewable Energy 2015;83:1066–75.
[33] Liu H, Tian HQ, Liang XF, Li YF. Wind speed forecasting approach using secondary decomposition algorithm and Elman neural networks. Appl Energy 2015;157:183–94.
[34] Liu H, Tian HQ, Li YF. Comparison of new hybrid FEEMD–MLP, FEEMD–ANFIS, wavelet packet-MLP and wavelet packet-ANFIS for wind speed predictions. Energy Convers Manage 2015;89:1–11.
[35] Salcedo-Sanz S, Muñoz-Bulnes J, Portilla-Figueras J, Del Ser J. One-year-ahead energy demand estimation from macroeconomic variables using computational intelligence algorithms. Energy Convers Manage 2015;99: 62–71.
[36] Salcedo-Sanz S, Pastor-Sánchez A, Prieto L, Blanco-Aguilera A, García-Herrera R. Feature selection in wind speed prediction systems based on a hybrid coral reefs optimization–extreme learning machine approach. Energy Convers Manage 2014;87:10–8.
[37] Lombardi AM. Some reasoning on the RELM-CSEP likelihood-based tests. Earth, Planets and Space 2014;66:4.